COMPRESSIBLE TURBULENT REACTING FLOWS

(AFOSR Grant No. F49620-96-1-0106, Final Report)

Principal Investigators: F. A. Williams, P. A. Libby and S. Sarkar

Department of Mechanical and Aerospace Engineering
University of California San Diego, La Jolla, CA 92093-0411

1. INTRODUCTION

The primary objective of the research conducted under this grant is to advance fundamental understanding and prediction capabilities of reacting flows relevant to Air Force needs in high-speed airbreathing propulsion. The dynamical coupling among the turbulence, thermodynamic variables and fuel chemistry is not well-understood. Advanced simulations of prototypical shear flows and associated analytical tools are used here to understand and to model important aspects of this coupling.

The computational tools are primarily direct numerical simulation (DNS) and large eddy simulation (LES). In DNS, the conservation equations for a compressible, multi-species, reacting mixture are numerically solved to capture all dynamically important scales of turbulent motion without resort to any turbulence closure. In LES, filtered equations that represent the behavior of the 'large eddies' are simulated and the influence of the unresolved 'small eddies' modeled with an appropriate subgrid-scale (SGS) model. Both DNS and LES involve the numerical solution of unsteady, three-dimensional forms of the governing equations. LES requires fewer computational grid points than DNS and, provided that accurate SGS models are developed, can be used for high-Reynolds number flows. DNS has the advantage of giving results that do not depend on possible flaws in turbulence closures and, therefore, is best suited for developing new insights and uncovering new phenomena.

Th research accomplished as part of this grant has resulted in 19 publications and two Ph.D. theses.

2. THE COMPRESSIBLE, REACTING SHEAR LAYER

DNS has been used to study in detail the compressible, reacting shear layer and to discriminate among compressibility effects due to high-speed, variable density and exothermicity. The flow consists of hydrocarbon fuel and air streams with a relative shear which mix and react. Unlike previous simulations, large computational domains

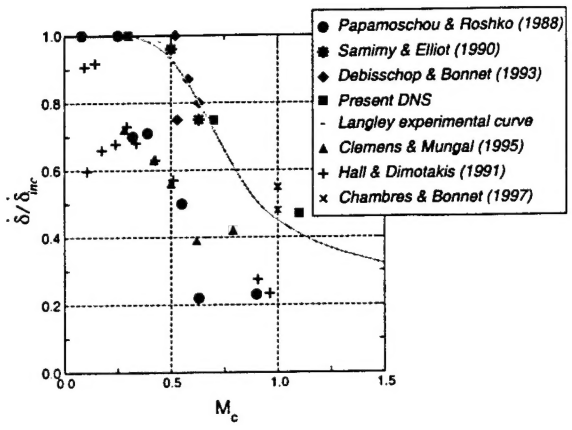

Figure 1: Dependence of the shear layer growth rate on the convective Mach number, M_c. The growth of the shear layer thickness, $\dot{\delta}$, is normalized by its incompressible value.

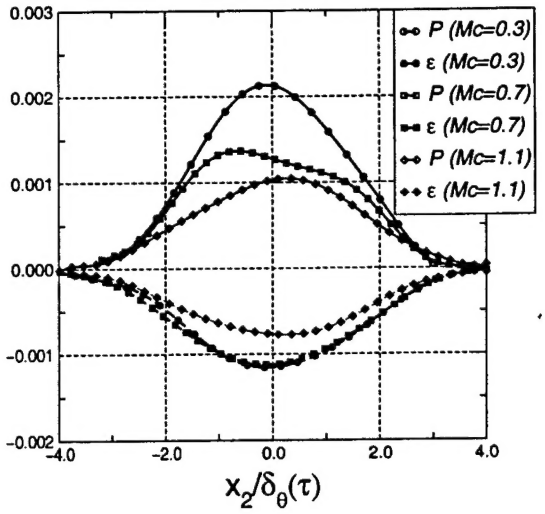

Figure 2: The dependence of turbulent kinetic energy production, P, and dissipation, ϵ on M_c. The production and dissipation are normalized using ΔU and δ_θ.

are used along with broadband initial fluctuations to allow evolution to the self-similar state. Indeed, it is found that qualitative differences in the turbulence structure and dynamics exist between the self-similar shear layer and the earlier-time, developing shear layer. Grids with up to 13 million points are used. The final Reynolds numbers, based in vorticity thickness, are large enough for turbulent flow, reaching values as large as 12,000. High-order discretizations are used to ensure numerical accuracy with fourth- and sixth-order compact schemes for the spatial derivatives and a third-order Runge Kutta scheme for time advancement. The integral length scales are sufficiently small compared to the dimensions of the computational box to have accurate large-scale representation, while the grid step is sufficiently small to resolve the small scales.

Highlights of our results are summarized below with further details available in articles [1, 2, 3, 4, 5, 6, 7, 8] and a Ph.D. thesis [9] resulting from this work.

2.1 The high-speed effect

The convective Mach number, $M_c = (U_1 - U_2)/(c_1 + c_2)$, is often used to characterize high-speed shear layers. Here U_1, c_1 denote the velocity and sound speed in the upper free stream, while U_2, c_2 refer to the lower stream. The dramatic reduction of shear layer growth rate with increasing M_c is well-known. As shown in Figure 1, our DNS results obtained with equal-density streams are in close agreement with the Langley

experimental curve and other data sets which use air-air streams. The experimental data points with reduced growth rates with respect to the Langley curve correspond to heterogeneous gases with unequal density.

With DNS, we are able to uncover a mechanism which accounts for the reduction in the shear layer growth rate with increasing Mach number. The decreased level of turbulent kinetic energy production (see Fig. 2) is found to be responsible for the reduction in question in agreement with the conclusion drawn by [10] from DNS of uniformly sheared flow. The normalized production has been also found to decrease with M_c in an independent study of the shear layer[11] and in the annular shear layer [12]. Fig. 2 shows that, while the normalized turbulent production, P, decreases with increasing Mach number, the turbulent dissipation, ϵ, does not decrease proportionally, resulting in a net decrease of turbulent kinetic energy.

Further examination of the Reynolds stress transport equations using the DNS database shows that a reduction in the pressure-strain term reduces the energy transfer from the streamwise component to the other components, thus decreasing the Reynolds shear stress and, thereby, the turbulent production, P. The pressure-strain term is responsible for transfer of energy among the three velocity components and is defined by $\Pi_{ij} = \overline{p'(\partial u_i'/\partial x_j + \partial u_j'/\partial x_i)}$, where p' is the pressure fluctuation and u_i' the velocity fluctuation. Fig. 3 shows that all components of the pressure-strain tensor, Π_{ij}, decrease with increasing M_c. The normalized pressure fluctuations (not shown) also decrease with increasing M_c.

An analysis to uncover the mechanism underlying the reduction in the pressure-strain term has been performed. In strictly incompressible flow, the instantaneous pressure has 'infinite' signal speed and satisfies a Poisson equation whose source is related to the velocity gradients. In the case of compressible flow, pressure fluctuations travel with the speed of sound, c_0. The consequence of a 'finite' signal speed on the pressure-strain term is studied analytically.

The following evolution equation for the pressure fluctuation p',

$$\frac{1}{c_o^2}\frac{D^2p'}{Dt^2} - \frac{\partial^2 p'}{\partial x_i \partial x_i} = \frac{\partial}{\partial x_i \partial x_j}\Big(\rho u_i u_j\Big)' \tag{1}$$

can be derived by taking the divergence of the momentum equation, and assuming that the isentropic relationship, $Dp/Dt = c_o^2 D\rho/Dt$, applies and that viscous terms are negligible. Such assumptions are reasonable for high-Reynolds number flows away from shocks and solid boundaries. Eq. (1) is now specialized to the center of the shear layer where the mean velocity is zero, $\partial\tilde{u}_1/\partial x_2 \simeq$ constant, and an analysis, assuming locally-

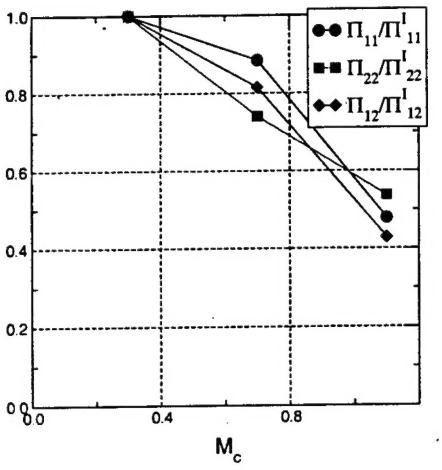

Figure 3: Dependence of components of the pressure-strain tensor, Π_{ij}, normalized by corresponding incompressible values, on M_c. Subscripts 1 and 2 denote streamwise and cross-stream directions, respectively

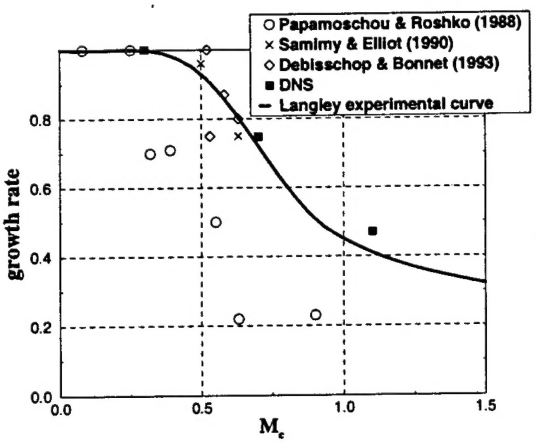

Figure 4: The performance of the new pressure-strain model in predicting the compressibility effect on the shear layer growth rate

homogeneous turbulence, is performed that involves two-point, two-time correlations. Details of the analysis are given in [1]. The result, for low Mach number, is

$$\frac{\Pi_{ij}}{\Pi_{ij}^I} = 1 - K_0 M_c^2 \tag{2}$$

which shows that Π_{ij} exhibits *monotone decrease* with M_c in agreement with the DNS results shown in Fig. 3.

The wave equation, Eq. (1), for the pressure is a useful approximation is consistent with the energy equation, if heat conduction and viscous dissipation terms are assumed negligible and the isentropic relation is assumed. However, since these assumptions are not physically supported when M_c is not small, at high Mach number, the general thermodynamic relation must be used,

$$\frac{Dp}{Dt} = \left(\frac{dp}{d\rho}\right)_s \frac{D\rho}{Dt} + \left(\frac{dp}{dS}\right)_\rho \frac{DS}{Dt} \tag{3}$$

where the first term on the r.h.s. is the 'acoustic' contribution and the second term is the 'entropy' contribution. Indeed, by taking the time derivative of Eq. (3) and using

the divergence of the momentum equation, a modified wave equation for the pressure fluctuation results, which involves entropy fluctuations and is valid for all Mach numbers. Analysis of the modified wave equation shows that $\Pi_{ij} \rightarrow const$, for large M_c. Thus, analysis provides functional forms for small and large Mach numbers.

A predictive model for the pressure-strain correlation which has the analytically predicted behavior at low and high Mach number is obtained by using the 'experimental' values of Π_{11} deduced from the Langley growth rate curve to determine the coefficients in the asymptotic solutions and using a exponential fitting function to approximate the difference at intermediate Mach numbers. The new pressure-strain model,

$$\frac{\Pi_{ij}}{\Pi_{ij}^I} = (1-c)\frac{1+aM_c^2 e^{-(2M_c-1/2)^2}}{1+bM_c^2} + c \tag{4}$$

for the compressibility effect on the pressure-strain term can provide the dependence of growth rate on M_c as shown in Fig. 4.

Based on analysis and DNS observations, the following mechanism is proposed to explain the fundamental property of compressible turbulence that results in the reduced growth rate of the shear layer. The *finite* speed of sound implies that the temporal decorrelation (over and above spatial decorrelation) between adjacent points becomes *additionally* important with increasing M_c. Consequently, the pressure-strain term decreases and the turbulence redistribution necessary to maintain shear-driven turbulence decreases so as to reduce the thickness growth rate.

The anisotropy of the Reynolds stresses, $R_{ij} = \overline{\rho u_i' u_j'}/\bar{\rho}$, is an important characteristic of the velocity fluctuations used in advanced modeling of turbulent flows. The tensor, $b_{ij} = R_{ij}/2K - \delta_{ij}/3$, where K is the turbulent kinetic energy is used to characterize Reynolds stress anisotropy. The effect of M_c on the anisotropy is controversial, with some investigations reporting a substantial increase of the anisotropy in the high-speed regime and others reporting negligible changes. Two important conclusions are drawn from our DNS. First, during its *initial* evolution, the anisotropy tensor is strongly affected by M_c such that larger magnitudes of the diagonal components of b_{ij} are measured for increasing M_c. Second, after sufficiently long time, the values of the anisotropy tensor approach asymptotic values only weakly dependent on M_c. The peak values of turbulence intensities and shear stress at the center of the shear layer can also be considered and indeed are preferable in comparing DNS with experimental data. The new results obtained by [13] who measure all three turbulence intensities as well as the Reynolds shear stress, and the older data of [14] are in good agreement with the present DNS.

2.2 Effect of density ratio

The convective Mach number has often been assumed to be the sole parameter that determines compressibility effects in the shear layer. However, there is significant scatter in Fig. 1 among the air-air data (Langley experimental curve, Elliot and Samimy (1990), Debisschop and Bonnet (1993), Chambres, Barre and Bonnet (1997)) and the other data sets which used gases with different densities. DNS is performed to investigate potential effects of the density ratio. The ratio of the freestream densities, $s = \rho_2/\rho_1$, is varied while the average density $\rho_0 = (\rho_1 + \rho_2)/2 = 0.7$ constant. The convective Mach number is also held fixed at $M_c = 0.7$. Values of $s = 1$, 4 and 8 are examined.

The momentum thickness defined by

$$\delta_\theta = \frac{1}{\rho_o \Delta u^2} \int_{-\infty}^{\infty} \bar{\rho}(\frac{\Delta u}{2} - \tilde{u}_1)(\frac{\Delta u}{2} + \tilde{u}_1) dx_2 \,. \tag{5}$$

and the vorticity thickness defined by

$$\delta_\omega = \Delta u / (\partial \tilde{u}_1 / \partial x_2)_{max} \tag{6}$$

are popular measures of the shear layer thickness. Here ΔU is the velocity difference across the shear layer and x_2 is the cross-stream coordinate. It is important to distinguish between these two thickness measures as will be shown subsequently. Note that for any variable ϕ, the density-weighted Favre average is denoted by $\tilde{\phi}$ while the unweighted average is denoted by $\bar{\phi}$.

The temporal growth rate of the vorticity thickness in a frame moving with the convection velocity is defined by

$$\dot{\delta}_\omega = \frac{1}{\Delta u} \frac{d\delta_\omega}{dt} \tag{7}$$

and, for the incompressible case,

$$\dot{\delta}_\omega = \frac{C_\delta}{2} \tag{8}$$

where C_δ is a nominal constant. As established in the previous section, C_δ decreases with M_c but here the influence of density ratio on C_δ is of interest. In the low-speed case, [15], based on limited low-speed, variable-density shear layer data, hypothesized that C_δ is independent of density ratio. Our results at $M_c = 0.7$ are shown in Table 1. It is clear that the influence of density ratio on C_δ is insignificant even in the high-speed regime.

On the other hand, the momentum thickness growth rate decreases systematically with departures of density ratio from its reference value of $s = 1$ as shown in Table 2.

Table 1: The influence of density ratio on the growth rate of the vorticity thickness

s	C_δ
1	0.117
4	0.137
8	0.125

Table 2: Density ratio effect on growth rate ratio.

s	DNS, $\dot{\delta}_\theta/\dot{\delta}_{\theta,1}$	Model, Eq. (9)
1	1.00	1.00
4	0.86	0.82
8	0.59	0.70

Self-similar profiles of the Reynolds shear stress are shown in Fig. 5. The peak values do not vary with density ratio, consistent with the insignificant change in vorticity thickness growth rate. However, the location of the peak Reynolds shear stress shifts to positive values of x_2/δ_θ along with the (approximately coincident) position of the dividing streamline. The location of the dividing streamline, $U = 0$, can be determined from the velocity profiles in Fig. 6. Also, from the density profiles in that figure it is clear that the location of the dividing streamline and the peak Reynolds shear stress lie in the low-density side of the shear layer. The *shift* of the center of the velocity profile, $U = 0$, with respect to the center of the density profile, $\rho = (\rho_1 + \rho_2)/2 = 0.7$, increases with density ratio as shown by Fig. 6. The DNS data are used to parameterize this shift by a quantity $a(s)$. This shift towards the low-density stream increases when s increases resulting in the systematic decrease of peak values of $\bar{\rho}R_{12}$ and therefore of the momentum thickness growth rate. An analysis has been carried out to explain this shift and yield the following model,

$$\frac{\dot{\delta}_\theta(s)}{\dot{\delta}_\theta(s=1)} = 1 - 0.4\lambda(s)a(s) \tag{9}$$

where $\lambda(s) = (s-1)/(1+s)$ and $a(s)$ is a parameter that determines the shift of the center of the mean velocity profile with respect to that of the mean density profile. Table 2 shows that Eq. (9) is a good approximation to the observed effect of density ratio on the momentum thickness growth rate.

2.3 Effect of heat release

Popular models of flow/chemistry interaction such as the unsteady laminar flamelet [19, 20] and the conditional moment method [21, 22, 23] are based on the knowledge of the statistics of two variables; a mixture fraction variable, ζ, that represents the state of mixing and a second variable, the scalar dissipation, χ, defined as $2D\nabla\zeta \cdot \nabla\zeta$, with D the mass diffusivity. These models attempt to simplify the coupling between the scales

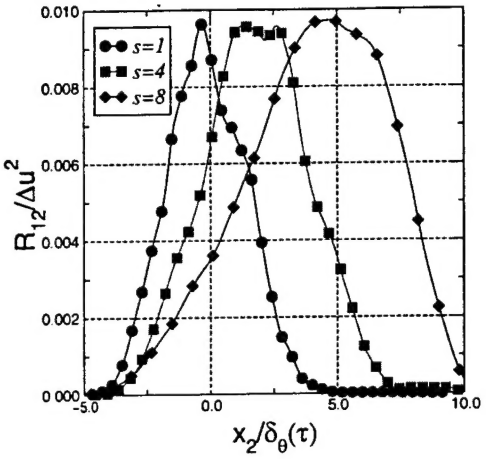

Figure 5: Self-similar profiles of Reynolds shear stress, R_{12}, for various density ratios. The cross-stream coordinate, x_2, is nondimensionalized with the momentum thickness.

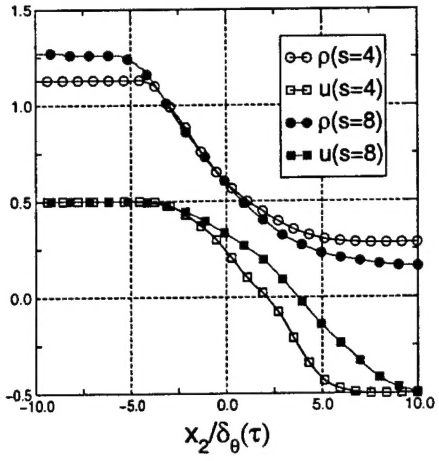

Figure 6: Self-similar profiles of the mean velocity and density. The center (where U = 0) of the mean velocity profile is shifted with respect to the center (where $\rho = 0.7$) of the mean density profile.

of turbulence and the several orders of magnitude smaller chemical scales. Since little is known on the effect of heat release on the mixture fraction and scalar dissipation, we have focussed our DNS analysis on these quantities.

For obtaining the leading-order effect of heat release it is not necessary to consider multi-step, finite rate chemistry. Thus, the single-step, infinitely fast irreversible combustion of methane with air is considered,

$$CH_4 + 2O_2 \rightarrow CO_2 + 2H_2O \tag{10}$$

The heat release is represented by $Ce = T_{ad}/T_0 - 1$, where T_{ad} is the adiabatic flame temperature and T_0 is the reference freestream temperature. A stoichiometric mixture fraction value of $\zeta_s = 0.2$ was fixed by diluting the fuel stream with nitrogen. In addition to the value of $Ce = 7$ corresponding to the chosen stoichiometry, a case with $Ce = 3.5$ with the heat release constrained to half the actual value is also considered.

The probability density function (pdf), $P(\zeta;\eta)$, of the scalar, ζ, is a function of the normalized cross-stream coordinate, $\eta = x_2/\delta_\omega$, in the self-similar shear layer. Figure 7(a) shows the scalar pdf, $P(\zeta;\eta)$, at $\eta = 0.2$ (average position of the flame) for the turbulent shear layer in cases $Ce = 0$, 3.5 and 7. The values of $P(\zeta = \zeta_s;\eta = 0.2)$ in

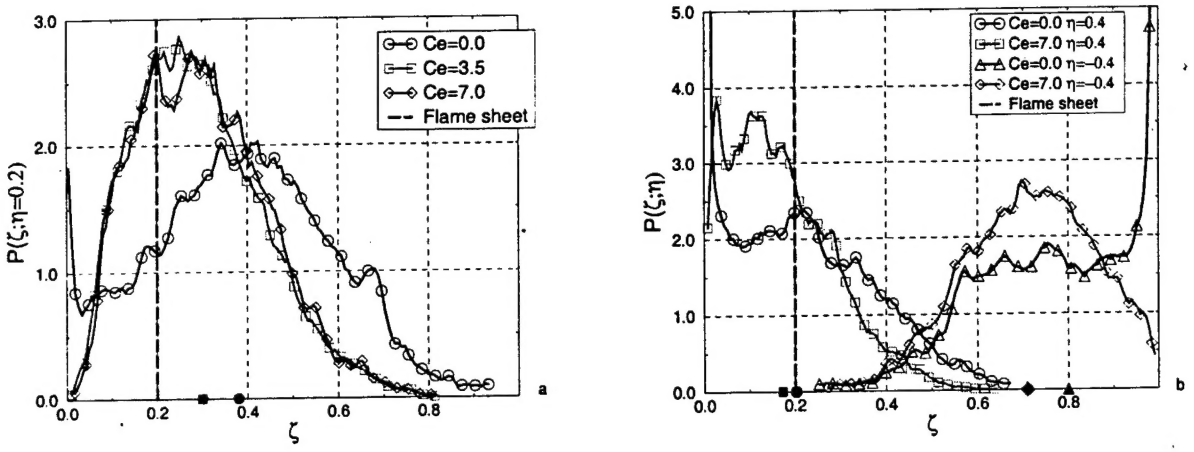

Figure 7: Scalar pdf (a) $Ce = 0$, 3.5 and 7 at $\eta = 0.2$ and (b) $\eta = \pm 0.4$. Here, $\eta = x_2/\delta_\omega$ is the normalized cross-stream coordinate.

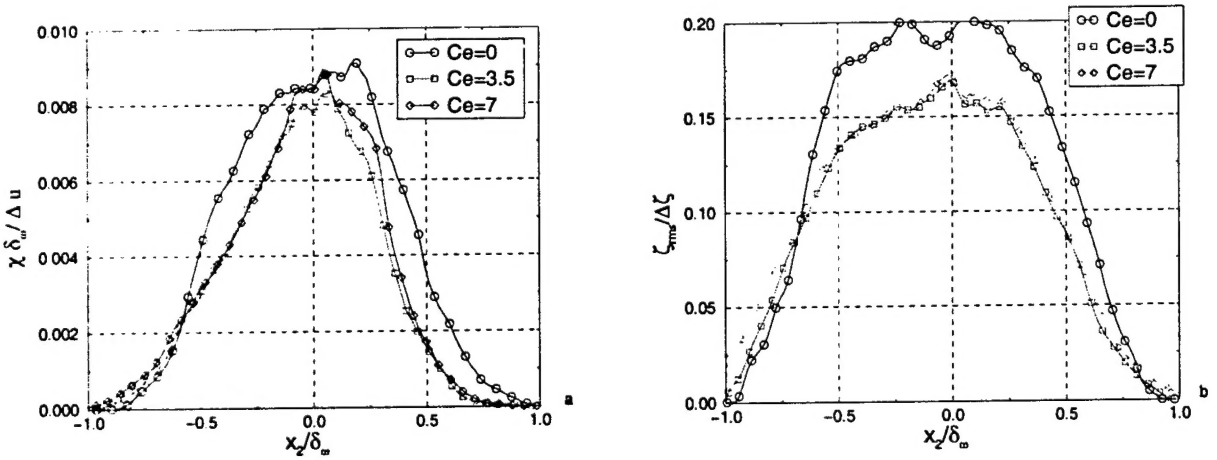

Figure 8: Scalar dissipation (a) and scalar r.m.s (b) for $Ce = 0$, 3.5 and 7.

both cases with heat release are about twice the value for the case without heat release. Figure 7(b) shows the scalar pdf at $\eta = \pm 0.4$. The pdf is no longer symmetric, since the stoichiometric value, $\zeta_s = 0.2$, introduces an asymmetry in the mixing layer. Another feature of the reacting cases is that external intermittency is suppressed. These changes should be considered when developing models for reacting flows. Moreover, the use of pdf measurements that correspond to non-reactive flows could lead to incorrect predictions.

Figure 8(a) shows the unconditional scalar dissipation, χ, normalized by vorticity thickness, as a function of the coordinate η. It can be seen that, although the non-reacting and reacting cases have similar profiles when δ_ω is used as the scaling parameter, there is some reduction in the thickness of the unconditional scalar dissipation profile when there is heat release. Figure 8(b) shows profiles of r.m.s (root mean square) scalar fluctuations for $Ce = 0$, 3.5 and 7. The levels of scalar r.m.s with heat release are lower than the values measured in the case without heat release.

The pdf of scalar dissipation conditioned on scalar mass fraction has a complex behavior in the reacting shear layer, a behavior which is currently being analyzed.

3. REDUCED CHEMISTRY FORMULATIONS

The structure of hydrogen-air diffusion flames in conditions typical of high-speed propulsion applications is studied with detailed and reduced chemistry mechanisms [16]. Pressures ranging from 0.25 atm to 10 atm, fuel stream temperatures ranging from 300 K to 600 K, and air temperatures from 500 K to 1500K are considered. It is found that a 21-step detailed kinetic mechanism can describe the structures, extinction and ignition of hydrogen-air diffusion flames over this range of conditions. More importantly, the efficacy of reduced mechanisms is examined in this study. A four-step mechanism based on steady state approximations for HO_2 and H_2O_2 gives essentially the same results as the detailed mechanism. A three-step mechanism, based on an additional steady-state approximation for OH, and a two-step mechanism, based on additional steady-state approximations for both OH and O is also evaluated. Both mechanisms, especially the three-step variant, are found to give acceptable predictions of ignition, extinction and heat-release, but do not predict radical concentrations.

A three-step reduced mechanism for hydrogen/oxygen combustion consists of a fast fuel-consumption step,

$$3H_2 + O_2 \rightarrow 2H_2O + 2H$$

together with two recombination steps

$$H + H \rightarrow H_2$$
$$2H_2 + O_2 \rightarrow 2H_2O\,.$$

The above mechanism is valid for strain conditions ranging from weakly strained flames to near extinction. Using the above mechanism with explicit reaction rate terms in DNS or LES is problematical because of the fast fuel-consumption step. Therefore, generalized coupling functions have been developed to give conservation equations that contain explicitly *only* the slow radical recombination rate while the fast fuel-consumption step is treated with the new coupling functions that, by virtue of being continuous functions, allow discrete differentiation, without any special techniques, in a simulation. Species diffusivities that differ from the thermal diffusivity are permitted. The mathematical model corresponds to a reaction sheet at which fuel is consumed in a diffusion-controlled fashion, yet allowing finite-radical recombination. Good results of the laminar flame structure are obtained by [17] with this formulation when applied to a hydrogen-air laminar mixing layer with free-stream temperatures above the crossover temperature corresponding to the second explosion limit.

Generalized coupling functions derived from a three-step reduced mechanism for the combustion of methane [18] are currently being evaluated for application in DNS.

4. THE TURBULENT JET: DNS

Turbulent plane jets are prototypical free shear flows of practical interest in propulsion and other applications. While considerable experimental research has been performed on planar jets, very few computational studies exist. Our work is the first computational study of a spatially-developing turbulent jet utilizing DNS. Comparisons of two- and three-dimensional simulations [24, 25, 26] show the inadequacy of the former. The development of the velocity and scalar field including successful comparison with experimental data is discussed in [27] while the effect of nozzle conditions is reported in [28]. A Ph.D. thesis [29] has also resulted from these studies.

The discussion here is limited to some features of the scalar field development in a turbulent jet with initial Reynolds number, $Re_h = 3000$, that increases to $Re_h = 4700$ at the outflow. Here, $Re_h = U_j h/\nu$ is based on the uniform jet exit velocity, U_j, and the nozzle height, h. Figures 9 and 10 show instantaneous isocontours of the passive scalar in an xy-plane (side section) and in a xz-plane (top section), respectively. The xz-plane shown is at a station $y/h = 0.467$ which is just below the upper shear layer at the inflow.

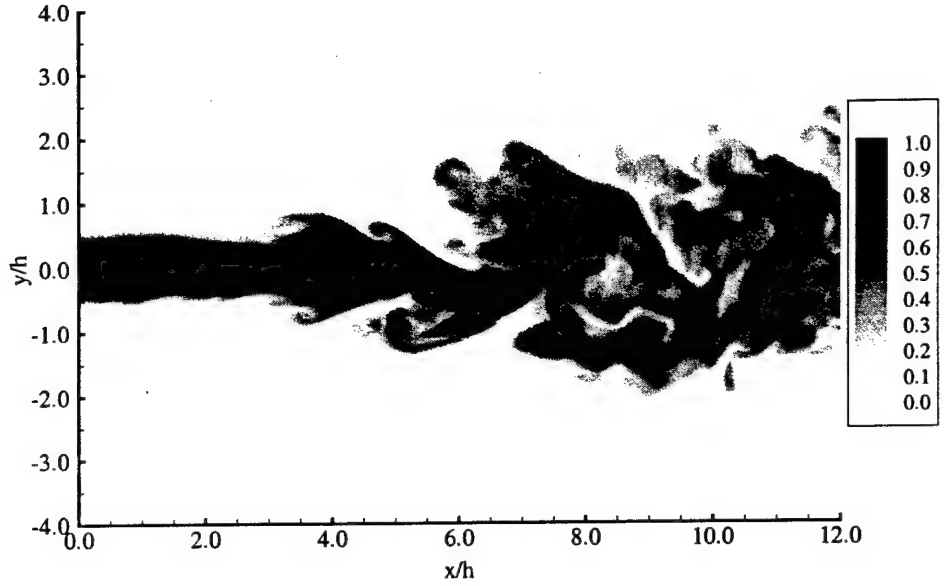

Figure 9: Instantaneous passive scalar contours on an xy-plane, $z = 0.0$. The nozzle height is denoted by h.

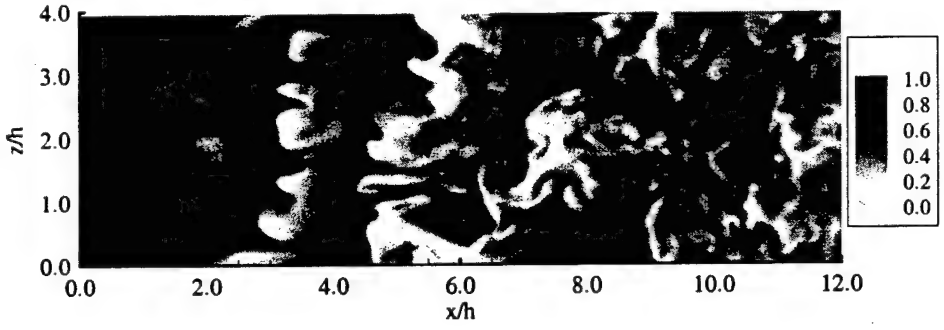

Figure 10: Instantaneous passive scalar contours on a xz-plane just below the upper shear layer, $y/h = 0.44$.

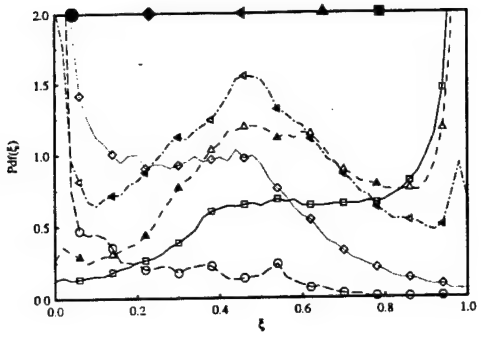

Figure 11: Variation of the probability density function of the passive scalar across the jet at $x/h = 7.0$. The cross-stream coordinate, y, is normalized by the scalar half-width, δ_ξ. Symbols: $\square$ $y/\delta_\xi = 0.00$, $\triangle$ $y/\delta_\xi = 0.43$, $\triangleleft$ $y/\delta_\xi = 0.87$, $\Diamond$ $y/\delta_\xi = 1.30$, $\bigcirc$ $y/\delta_\xi = 1.74$.

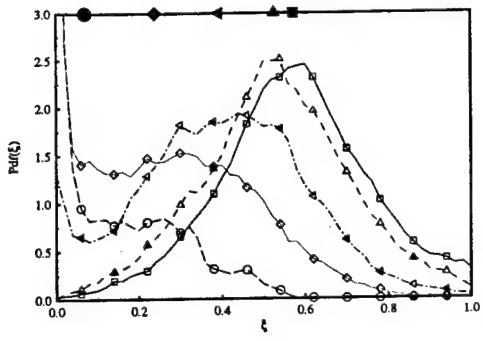

Figure 12: Variation of the probability density function of the passive scalar across the jet at $x/h = 11.5$. Symbols: $\square$ $y/\delta_\xi = 0.00$, $\triangle$ $y/\delta_\xi = 0.38$, $\triangleleft$ $y/\delta_\xi = 0.72$, $\Diamond$ $y/\delta_\xi = 1.07$, $\bigcirc$ $y/\delta_\xi = 1.45$.

At this lateral station, the inflow fluid is predominately jet fluid. In these figures, white indicates pure coflow fluid, $\widetilde{\xi} = 0.0$, while black indicates pure jet fluid, $\widetilde{\xi} = 1.0$. The jet column (almost pure jet fluid) is clearly evident in figure 9 and extends until $x/h = 5.0$ where it begins to break down. Shear layer and jet instabilities that have large spanwise extent (see Fig. 10) are evident in the initial region, $0 < x/h < 5$. Further downstream, small-scale structures with limited spanwise coherence dominate.

The scalar pdf's in turbulent jets have been a subject of some controversy. Figure 11 shows the scalar pdf's across the jet at the station $x/h = 7.0$. At this station, the probability density functions for $y/\delta_\xi = 0.43$, 0.87 and 1.30 are decidedly *non-marching*. While the mean scalar values, solid shaded symbols at the top of the plot, vary strongly for $0.43 \leq y/\delta_\xi \leq 1.30$, the central peak in the pdf's does *not* march, remaining stationary at scalar values $\xi \approx 0.5$. At each of these lateral stations there is a second strong peak in the probability density function corresponding to either pure jet fluid, $y/\delta_\xi = 0.43$, or pure coflow fluid, $y/\delta_\xi = 1.30$, or both $y/\delta_\xi = 0.87$. The probability density functions at $y/\delta_\xi = 0.0$ and 1.74 are quite broad and show a dominant peak of pure jet and pure coflow fluid, respectively. The non-marching pdf's at this streamwise station, $x/h = 7.0$, indicates that, in this region of the jet, mixing is dominated by the large-scale engulfing of fluid.

Figure 12 shows the probability density functions for the passive scalar field further

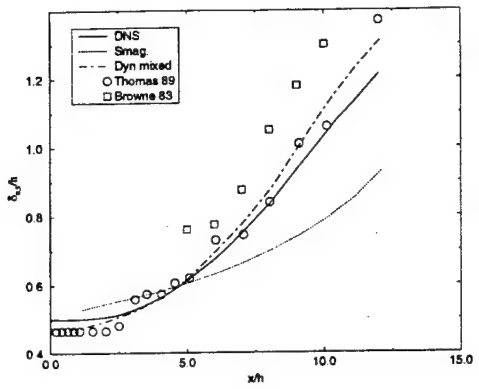

Figure 13: Evolution of the jet half-width in LES.

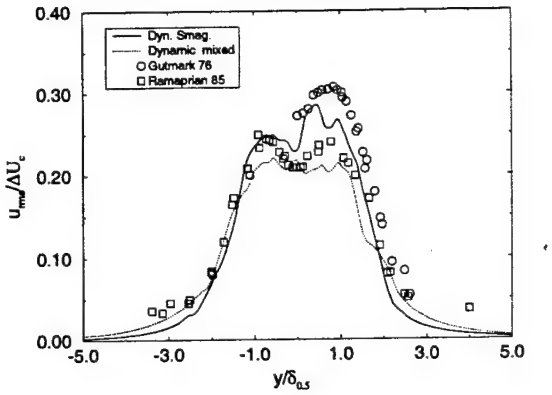

Figure 14: Profiles of streamwise turbulence intensity in LES.

downstream in the jet, $x/h = 11.5$, after the fluctuating velocity and scalar fields approach self-similarity. At this station, the PDF at the jet centerline no longer shows a strong peak corresponding to pure jet fluid, $\xi = 1.0$, implying that small-scale mixing has eliminated the presence of strong patches of unmixed jet fluid. The probability density functions at $y/\delta_\xi = 0.0$ and 0.38 exhibit "marching" type behavior at this streamwise station. There is a single peak in the PDF which marches along with the mean value of the passive scalar at that lateral location. Near the outer edges of the jet, there is a secondary peak corresponding to pure coflow fluid, suggesting intermittent, large-scale entrainment.

5. THE TURBULENT JET; LES

Large eddy simulations of a spatially developing jet have been performed [30] and three different subgrid stress models compared: the standard Smagorinsky model, the dynamic Smagorinsky model and the dynamic mixed model. A set of simulations at a low Reynolds number, $Re_d = 3,000$ enables comparisons with our previous DNS [27]. Then simulations are performed at a higher Reynolds number, $Re_d = 30,000$, more typical of engineering applications. Fig. 13 shows the evolution of the jet half-width. The standard Smagorinsky model is much too dissipative, while the other two models compare well with both DNS and experiments. Fig. 14 shows that, in the high Reynolds number jet, both the mixed and dynamic Smagorinsky models give turbulent intensity profiles consistent with experimental data.

Our *a priori* tests using the exact subgrid stresses obtained by filtering the DNS

jet data, show that the subgrid shear stress is severely underpredicted by the dynamic Smagorinsky model. On the other hand, surprisingly, the dynamic Smagorinsky model provides satisfactory overall results concerning flow statistics in *a posteriori* calculations, as shown by Fig. 13 and Fig. 14. Terms in the equation for streamwise velocity, U_1, are examined to understand this apparent contradiction. The dominant balance is found to be between mean convection and the transverse gradient of the *sum* of the resolved Reynolds shear stress and the unresolved SGS stress. After examination of the mean momentum balance, it is found that the sum of the resolved and subgrid shear stress is similar with both models, thus explaining their similar performance.

We are currently evaluating the ability of LES with subgrid scalar transport models to predict the evolution of mean, r.m.s. and pdf's of the scalar. Also, our new developments [31] in LES of nonequilibrium turbulent flows will be tested to predict the well-known sensitivity of jets to different coflow speeds, a difficult problem for RANS calculations.

6. COUETTE FLOWS AND RELATED STUDIES

A study of extinction by wall cooling and the influence of compressibility, heat transfer and shear on the rate of creation of product in laminar Couette flow [32] has resulted from the research conducted as part of this grant. In addition to being of fundamental interest, this contribution provides the basis for development of extended flamelet models, i.e., models applicable to high-speed turbulent reacting flows. One of the fundamental problems in the modeling of such flows relates to the treatment of fluctuating pressure gradients which, although neglected in previous theories, have been found to be important in recent DNS studies. In [33] a revised theory of premixed turbulent combustion involving a new model for such fluctuating gradients is developed and applied to turbulent reactant streams impinging on a wall, a flow for which a limited amount of accurate data on first and second moment quantities is available. Excellent agreement between theory and experiment is achieved. Particularly impressive is the agreement with respect to the mean axial flux.

Suggested by this success is a revisiting of the theory of turbulent flames normal to an oncoming reactant stream. The hope here is that, depending on the intensity of the turbulence in the stream relative to the laminar flame speed, a measure of the chemical kinetic rate of the mixture, we shall predict either countergradient or gradient transport. It is now known from both DNS results and experiment that under conditions of intense turbulence the countergradient transport seen so frequently in computations and experiment reverts to gradient form. This transition has never been predicted by a moment method, but it is hoped that the new model for fluctuating pressure gradients

will permit such a prediction.

As a follow on to these studies, models for the mean rate of creation of products are being currently examined; there are many such models, but they are never critically assessed by themselves. However, in our studies of flames in stagnating turbulence, this separation can be readily made, and each chemistry model assessed independently.

References

[1] C. Pantano and S. Sarkar, "A study of compressibility effects in the high-speed turbulent shear layer using direct simulation, " *J. Fluid Mech.*, submitted (1999).

[2] S. Sarkar and C. Pantano, " Contributions of DNS to the investigation of compressible, turbulent shear flows," Direct and Large-Eddy Simulation III, eds. P. R. Voke, N. D. Sandham and L. Kleiser, Kluwer Academic Publishers (1999).

[3] C. Pantano and S. Sarkar, "Compressibility effects in the high-speed, reacting shear layer," Turbulence and Shear Flow-I, eds. S. Banerjee and J. K. Eaton, 53-58 (1999).

[4] C. Pantano and S. Sarkar, "Scalar mixing in the turbulent reacting shear layer," Proceedings, 8th European Conference on Turbulence, Barcelona, pp. 4 (2000).

[5] C. Pantano, S. Sarkar and F. A. Williams, "The transport and mixing of a reactive scalar in non-premixed flames," in preparation (2000).

[6] S. Sarkar and C. Pantano, "Variable density effects in the high-speed turbulent reacting shear layer," Invited Lecture, International conference on variable density flows, Banyuls, France (2000).

[7] S. Sarkar, "On density and pressure fluctuations in uniformly sheared compressible flow," IUTAM Symposium on Variable Density Low-Speed Flows, Marseille, July 1996.*Fluid Mechanics and its Applications*, **41**, eds., L. Fulachier, J. L. Lumley, and F. Anselmet, Kluwer Academic Publishers, Dordrecht, 1997.

[8] G. Balakrishnan, S. Sarkar and F. A. Williams, "Direct numerical simulation of diffusion flames with large heat release in compressible homogeneous turbulence," AIAA 95-2375, *31st AIAA/ASME/SAE/ASEE Joint Propulsion Conference*, San Diego, July 1995.

[9] C. Pantano, "A study of the compressible turbulent reacting shear layer using direct numerical simulation," Ph. D. thesis, UC San Diego (2000).

[10] S. Sarkar, "The stabilizing effect of compressibility in turbulent shear flow", *J. Fluid Mech.* **282**, pp. 163–186 (1995).

[11] A. Vreman, N. Sandham, & K, Luo, "Compressible mixing layer growth rate and turbulence characteristics", *J. Fluid Mech.* **320**, pp. 235–258 (1996).

[12] J. Freund, P. Moin, & S. Lele, "Compressibility effects in a turbulent annular mixing layer", Stanford Report No. TF-72 (1997).

[13] O. Chambres, S. Barre, & J. Bonnet, "Detailed turbulence characteristics of a highly compressible supersonic turbulent plane mixing layer", *J. Fluid Mech.* submitted (1998).

[14] G. Elliot, & M. Samimy, "Compressibility effects in free shear layers", *Phys. Fluids A* **2** (7), pp. 1231–1240 (1990).

[15] G. Brown, "The Entrainment and Large Structure in Turbulent Mixing Layers", *5th Australasian Conf. on Hydraulics and Fluid Mechanics* pp. 352–359 (1974).

[16] G. Balakrishnan, M. D. Smooke and F. A. Williams, "A numerical investigation of extinction and ignition limits in laminar nonpremixed counterflowing hydrogen-air streams for both elementary and reduced chemistry, " *Combust. Flame*, **102**, 329-340 (1995).

[17] A. L. Sanchez, A. Linan and F. A. Williams, "A generalized Burke-Schumann formulation for hydrogen-oxygen diffusion flames maintaining partial equilibrium of the shuffle reactions, " *Combust. Sci. Tech.*, **123**, 317-345 (1997).

[18] F. A. Williams, "Formulations for turbulent diffusion flames with reduced chemistry, *Combust. Sci. Tech.*, Japanese Edition, **6**, 27-46 (1998).

[19] N. Peters, "Laminar flamelet concepts in turbulent combustion," *Twentyfirst Symp. (Intl.) on Combustion*, 1231-1250 (1986).

[20] H. Pitsch, M. Chen, and N. Peters, "Unsteady flamelet modeling of turbulent hydrogen-air diffusion flames," *Twentyseventh Symposium (Intl.) on Combustion*, 1057-1064 (1998).

[21] A. Klimenko, "Multicomponent diffusion of various admixtures in turbulent flow," *Fluid Dynamics*, **25**, 3-10 (1990)

[22] R. W. Bilger, "Conditional moment closures for turbulent reacting flows, " *Phys. Fluids*, **5**, 436-444 (1993).

[23] A. Y. Klimenko and R. W. Bilger, "Conditional moment closure for turbulent combustion," *Prog. Energy Combust. Science*, **25**, 595-687 (1999).

[24] S. Stanley and S. Sarkar, "Simulations of spatially developing two-dimensional shear

layers and jets," *Theor. Comput. Fluid Dyn.*, **9**, 121-147 (1997).

[25] S. A. Stanley and S. Sarkar, "Simulations of spatially developing plane jets," *AIAA Paper 97-1922*, 28th AIAA Fluid Dyn. Conf. (1997).

[26] S. Stanley and S. Sarkar, "Simulations of spatially developing plane shear layers and jets," *15th Intl. Conference on Numerical Methods in Fluid Dynamics*, Lecture Notes in Physics, **490**, 418-423 P. Kutler, J. Flores, J. -J. Chattot (Eds.), Springer-Verlag (1997).

[27] S. A. Stanley and S. Sarkar, "A study of the flowfield evolution and mixing in a planar turbulent jet using direct numerical simulation, " *J. Fluid Mech.*, submitted (1999).

[28] S. A. Stanley and S. Sarkar," Direct numerical simulation of the developing region of turbulent planar jets," *AIAA Paper 99-0288*, 37th Aerospace Sciences Meeting, Reno, January1999.

[29] S. A. Stanley," A computational study of spatially evolving turbulent plane jets," Ph.D. thesis, UC San Diego (1998)

[30] C. Le Ribault, S. Sarkar and S. A. Stanley, "Large eddy simulation of a plane jet," *Phys. Fluids*, **11**, 3069-3083 (1999).

[31] L. Shao, S. Sarkar, and C. Pantano, "On the relationship between the mean flow and subgrid stresses in LES of turbulent shear flows," *Phys. Fluids*, **11(5)**, 1229-1248 (1999).

[32] K. N. C. Bray, M. Champion and P. A. Libby, "Premixed combustion in laminar Couette flow-extinction and mass burning rate," *Combust. Flame*, **118**, 633-650 (1999).

[33] K. N. C. Bray, M. Champion and P. A. Libby, " Premixed flames in stagnating turbulence. Part IV - A new theory for the Reynolds stresses and Reynolds fluxes and exploited in impinging flows, " *Combust. Flame*, **120** 1-18 (2000).

PIADC Data

Faculty: Profs. Forman Williams, Paul Libby and Sutanu Sarkar

Postdocs: Dr. G. Balakrishnan, Dr. L. Shao, Dr. C. Le Ribault

Ph.D. students: Carlos Pantano, Scott Stanley

Publications:

1. G. Balakrishnan, M. D. Smooke and F. A. Williams, "A numerical investigation of extinction and ignition limits in laminar nonpremixed counterflowing hydrogen-air streams for both elementary and reduced chemistry, " *Combust. Flame*, **102**, 329-340 (1995).
2. G. Balakrishnan, S. Sarkar and F. A. Williams, "Direct Numerical Simulation of Diffusion Flames with Large Heat Release in Compressible Homogeneous Turbulence," AIAA 95-2375, *31st AIAA/ASME/SAE/ASEE Joint Propulsion Conference*, San Diego, July 1995.
3. S. Sarkar, "On density and pressure fluctuations in uniformly sheared compressible flow," IUTAM Symposium on Variable Density Low-Speed Flows, Marseille, July 1996,*Fluid Mechanics and its Applications*, **41**, eds., L. Fulachier, J. L. Lumley, and F. Anselmet, Kluwer Academic Publishers, Dordrecht, 1997.
4. A. L. Sanchez, A. Linan and F. A. Williams, "A generalized Burke-Schumann formulation for hydrogen-oxygen diffusion flames maintaining partial equilibrium of the shuffle reactions, " *Combust. Sci. Tech.*, **123**, 317-345 (1997).
5. S. Stanley and S. Sarkar, "Simulations of spatially developing two-dimensional shear layers and jets," *Theor. Comput. Fluid Dyn.*, **9**, 121-147 (1997).
6. S. A. Stanley and S. Sarkar, "Simulations of spatially developing plane jets," *AIAA Paper 97-1922*, 28th AIAA Fluid Dyn. Conf. (1997).
7. S. Stanley and S. Sarkar, "Simulations of spatially developing plane shear layers and jets," *15th Intl. Conference on Numerical Methods in Fluid Dynamics*, Lecture Notes in Physics, **490**, 418-423 P. Kutler, J. Flores, J. -J. Chattot (Eds.), Springer-Verlag (1997).
8. S. A. Stanley and S. Sarkar, "A study of the flowfield evolution and mixing in a planar turbulent jet using direct numerical simulation, " *J. Fluid Mech.*, submitted (1999).
9. S. A. Stanley and S. Sarkar," Direct numerical simulation of the developing region of turbulent planar jets," *AIAA Paper 99-0288*, 37th Aerospace Sciences Meeting, Reno, January1999.
10. S. A. Stanley," A computational study of spatially evolving turbulent plane jets," Ph.D. thesis, UC San Diego (1998)
11. L. Shao, S. Sarkar, and C. Pantano, "On the relationship between the mean flow and subgrid stresses in LES of turbulent shear flows," *Phys. Fluids*, **11(5)**, 1229-1248 (1999).
12. C. Le Ribault, S. Sarkar and S. A. Stanley, "Large eddy simulation of a plane jet," *Phys. Fluids*, **11**, 3069-3083 (1999).

13. C. Pantano and S. Sarkar, "A study of compressibility effects in the high-speed turbulent shear layer using direct simulation, " *J. Fluid Mech.*, submitted (1999).

14. S. Sarkar and C. Pantano, " Contributions of DNS to the investigation of compressible, turbulent shear flows," Direct and Large-Eddy Simulation III, eds. P. R. Voke, N. D. Sandham and L. Kleiser, Kluwer Academic Publishers (1999).

15. C. Pantano and S. Sarkar, "Compressibility effects in the high-speed, reacting shear layer," Turbulence and Shear Flow-I, eds. S. Banerjee and J. K. Eaton, 53-58 (1999).

16. C. Pantano and S. Sarkar, "Scalar mixing in the turbulent reacting shear layer," Proceedings, 8th European Conference on Turbulence, Barcelona, pp. 4 (2000).

17. K. N. C. Bray, M. Champion and P. A. Libby, "Premixed combustion in laminar Couette flow-extinction and mass burning rate," *Combust. Flame*, **118**, 633-650 (1999).

18. K. N. C. Bray, M. Champion and P. A. Libby, " Premixed flames in stagnating turbulence. Part IV - A new theory for the Reynolds stresses and Reynolds fluxes and exploited in impinging flows, " *Combust. Flame*, **120** 1-18 (2000).

19. C. Pantano, S. Sarkar and F. A. Williams, "The transport and mixing of a reactive scalar in non-premixed flames," in preparation (2000).

20. S. Sarkar and C. Pantano, "Variable density effects in the high-speed turbulent reacting shear layer," Invited Lecture, International conference on variable density flows, Banyuls, France (2000).

21. C. Pantano, "A study of the compressible turbulent reacting shear layer using direct numerical simulation," Ph. D. thesis, UC San Diego (2000).

Technology Transfer:

Performers: Drs. P. A. Libby and F. A. Williams
University of California, San Diego
(858)-534-5492

Customer: Dr. Alan Turan
Solar Turbines
San Diego, CA
(619) 544-2810

Result: Theory of partially premixed turbulent combustion applicable to gas turbines.

Application: Improve design of gas turbines to lower emissions.

Honors/Awards:

Paul A. Libby, elected to National Academy of Engineering, 1999.

Forman A. Williams, Best Paper Award, Combustion and Fuels Committee, IGTI, ASME, 1999.

Forman A. Williams, Thermal Engineering Award for International Activity, Japan Society of Mechanical Engineering, 1999.

REPORT DOCUMENTATION PAGE

1. AGENCY USE ONLY (*Leave Blank*)	2. REPORT DATE	3. REPORT TYPE AND DATES COVERED
	17 March 2000	Final Report 15 March 1996 – 31 October 1999

4. TITLE AND SUBTITLE

Compressible Turbulent Reacting Flows

5. FUNDING NUMBERS

PE - 61102F
PR - 2308
SA-BX
G - F49620-96-1-0106

6. AUTHORS

F.A. Williams, P.A. Libby and S. Sarkar

7. PERFORMING ORGANIZATION NAME(S) AND ADDRESS(ES)

University of California, San Diego
9500 Gilman Drive
La Jolla, CA 92093-0411

8. PERFORMING ORGANIZATION REPORT NUMBER

9. SPONSORING / MONITORING AGENCY NAME(S) AND ADDRESS(ES)

AFOSR/NA
801 N. Randolph Road, Room 732
Arlington, VA 2203-1977

10. SPONSORING / MONITORING AGENCY REPORT NUMBER

11. SUPPLEMENTARY NOTES

12a. DISTRIBUTION / AVAILABILITY STATEMENT

Approved for public release; distribution is unlimited

12b. DISTRIBUTION CODE

13. ABSTRACT *(Maximum 200 words)*

Research was conducted under this grant to advance fundamental understanding and predictive models of turbulent reacting flows relevant to Air Force needs in high-speed propulsion. Advanced computational schemes including direct numerical simulation (DNS) and large eddy simulation (LES) were used in addition to turbulent combustion theory. Reduced chemical mechanisms for hydrogen-air combustion were developed and tested. Specific flows investigated include the reacting shear layer and the jet. A new mechanism that relates the reduction in fuel/oxidant mixing in high-speed flows to the inhibited communication of pressure signals was proposed. A resulting compressibility model was found to give good predictions. Both mean density changes and Mach number were found to affect the flow development in high-speed combustion. It was found that the transport and molecular mixing of reactive scalars are substantially affected by heat release and must be accounted for in closures of turbulence/chemistry interaction. LES of a spatially-evolving jet were performed and successfully compared with our DNS and previous experiments. New subgrid scale models were developed for LES of nonequilibrium flows. The results obtained here should help improve current abilities to analyze and design propulsion systems that employ high-speed turbulent combustion.

14. SUBJECT TERMS

diffusion flames, turbulent flames, compressible combustion

15. NUMBER OF PAGES
18

16. PRICE CODE

17. SECURITY CLASSIFICATION OF REPORT	18. SECURITY CLASSIFICATION OF THIS PAGE	19. SECURITY CLASSIFICATION OF ABSTRACT	20. LIMITATION OF ABSTRACT
Unclassified	Unclassified	Unclassified	UL

NSN 7540-01-280-5500

Standard Form 298 (Rev. 2-89)
Prescribed by ANSI Std. Z39-1
298-102